Available online at www.sciencedirect.com
ScienceDirect
Journal of Molecular Catalysis A: Chemical 265 (2007) 1–8
JOURNAL OF MOLECULAR CATALYSIS A: CHEMICAL
www.elsevier.com/locate/molcata

Nanoclustered palladium(0) supported on a gel-type poly-acrylonitrile–*N*, *N*-dimethylacrylamide–ethylenedimethacrylate resin: Nanostructural aspects and catalytic behaviour

L. De Zan [a], D. Gasparovicova [b], M. Kralik [c,*], P. Centomo [a], M. Carraro [a], S. Campestrini [a], K. Jerabek [d,*], B. Corain [a,e,*]

[a] *Dipartimento di Scienze Chimiche, Via Marzolo 1, 35131 Padova, Italy*
[b] *Institute of Organic Chemistry, Catalysis and Petrochemistry, Department of Organic Technology, Slovak University of Technology, Radlinskeho 9, SK-812 37 Bratislava, Slovak Republic*
[c] *VUCHT j.s.c., Nobelova 34, SK-836 03 Bratislava, Slovak Republic*
[d] *Institute of Chemical Process Fundamentals, Czech Academy of Sciences, Prague-Suchdol, Czech Republic*
[e] *Istituto di Scienze e Tecnologie Molecolari, CNR, Sezione di Padova, Via Marzolo 1, 35131 Padova, Italy*

Received 3 August 2006; received in revised form 4 September 2006; accepted 14 September 2006
Available online 16 September 2006

Abstract

Gel-type resin poly-acrylonitrile (30 mol%)–*N*,*N*-dimethylacrylamide (66 mol%)–ethylenedimethacrylate (4 mol%) (ADE) is obtained in very high yield with γ-rays-sustained polymerisation in mass. Water-swollen ADE microparticles react readily with $[PdCl_4^{2-}]$ in water to give a macromolecular complex likely to be Ⓟ-CN-$PdCl_3^-Na^+$. The material undergoes facile reduction to a Pd^0/ADE nanocomposite, in which a surprisingly non-homogeneous distribution of Pd^0 nanoclusters suggests a remarkable inhomogeneity in the distribution of the –CN groups through the polymer framework. This circumstance is attributed to a marked occurrence of a block-type polymerisation of the acrylonitrile leading to spheroidal domains that are particularly rich in –CN functionalities. Pd^0/ADE appears to be an active, re-usable, mechanically and chemically stable catalyst in the model hydrogenation reaction of cyclohexene in methanol under moderate conditions, carried out in batch reactors.

Keywords: Gel-type resins; Poly-acrylonitrile; Pd^0 co-ordination; Pd^0 nanoparticles; Hydrogenation and oxidation catalyst

1. Introduction

We have recently discovered that 4% cross-linked gel-type poly-acrylic resins are effective templates for the production of homogeneously dispersed size-controlled M^0 nanoclusters (M = Pd, Au), typically 3 nm in diameter [1–6] (Fig. 1). In this connection, we coined the term "template controlled synthesis" (TCS) [1].

Our rather extensive experience rests on structural and functional co-monomers such as DMAA (*N*,*N*-dimethylacrylamide, typical structural co-monomer), STY (styrene, occasional structural co-monomer), AA (acrylic acid), MA (methacrylic acid), MTEMA (2-(methylthio)ethylmethacrylate), SEMA (sulfoethyl methacrylate, a.k.a. methacryloxyethylsulfonic acid), VP (4-vinylpyridine), etc. (chosen functional co-monomers, Scheme 1), typically bearing a 4 mol% functional monomer and cross-linked with *N*,*N*′-methylenebisacrylamide 4 mol%.

We decided to test our TCS model with another significant acrylic co-monomer that bears a functional group exhibiting some ligating affinity to soft metal centers, such as acrylonitrile (hereafter referred to as AN). Moreover, in contrast with our previous protocol that relies on a 4–6 mol% of functional co-monomer, we designed a resin bearing ca. 30 mol% of AN, hereafter referred to as ADE. We report herein on the major micro- and nanostructural features of a Pd^0/ADE nanocomposite. We report also on its catalytic activity in the hydrogenation

* Corresponding authors.
E-mail address: benedetto.corain@unipd.it (B. Corain).

1381-1169/$ – see front matter © 2006 Elsevier B.V. All rights reserved.
doi:10.1016/j.molcata.2006.09.020

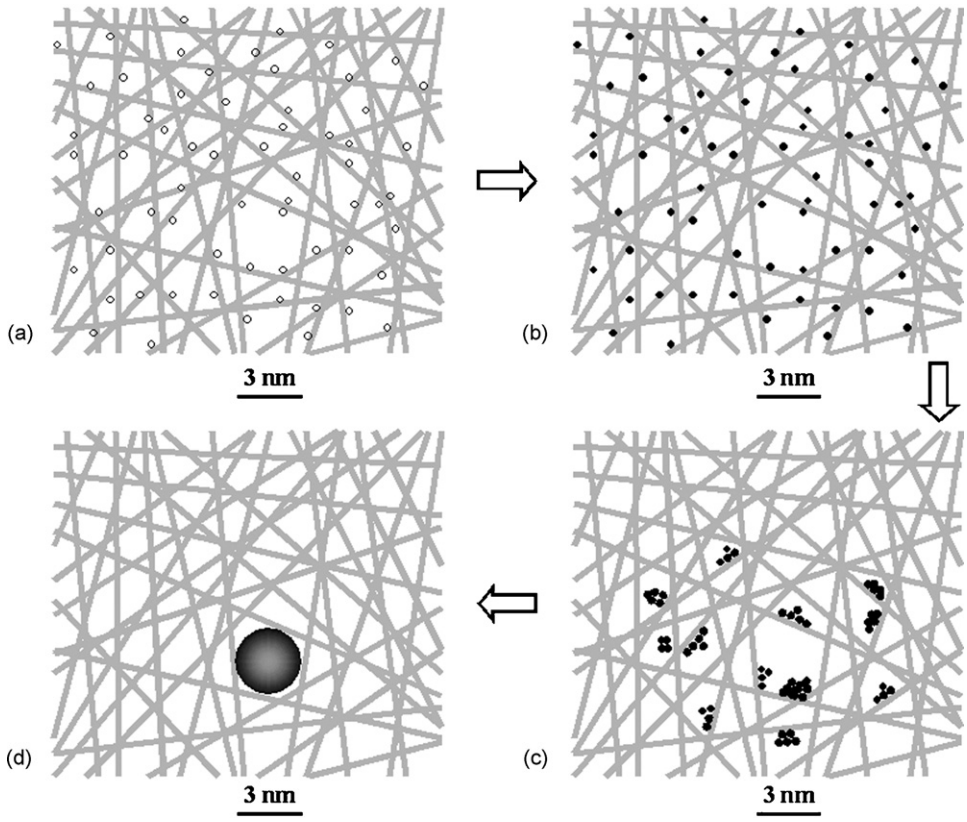

Fig. 1. Model for the generation of size-controlled metal nanoparticles inside metallated resins. (a) Pd^{II} is homogeneously dispersed inside the polymer framework; (b) Pd^{II} is reduced to Pd^0; (c) Pd^0 atoms start to aggregate in subnanoclusters; (d) a single 3 nm nanocluster is formed and "blocked" inside the largest mesh present in that "slice" of polymer framework, see text. (From Ref. [1], with permission.)

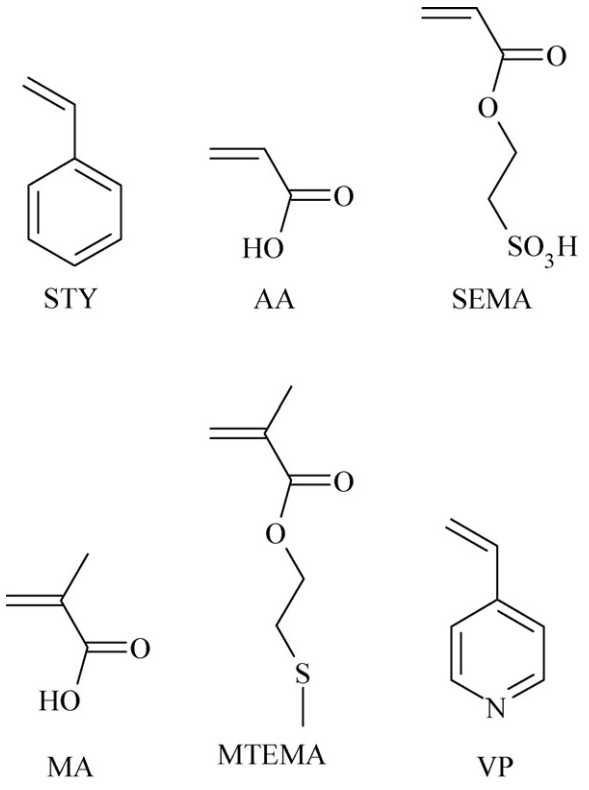

Scheme 1. Typical co-monomers used in these laboratories for preparing various designed gel-type functional resins [5–7] upon γ-rays-sustained polymerisation.

of cyclohexene (model reaction) in methanol and in the oxidation of benzyl alcohol and *n*-butanol with dioxygen in water. These last two substrates are chosen as reasonable paradigms of aromatic and aliphatic alcohols.

2. Experimental

2.1. Solvents and chemicals

From various commercial sources; they were used as received. Pd^0/EnCat was purchased from Aldrich, Pd^0/alumina was prepared as follows. Catalyst was prepared by the incipient wetness-impregnation of the support (gamma alumina, Aldrich, $s_{BET} = 164\ m^2/g$) using $Pd(NH_3)_4Cl_2$, dried, calcined at 400 °C and reduced by hydrogen in MeOH at 25 °C and pressure 6 bar, 1 h.

2.2. Apparatuses

XRMA. Cambridge Stereoscan 250 EDX PW 9800. *TEM*. PHILIPS CM 200 FEG with a Supertwin-Lens operated at an accelerating voltage of 200 keV. Lens parameters: $f = 1.7$ mm, Cs = 1.2 mm, Cc = 1.2 mm, giving a point resolution of 0.24 nm and a line resolution of 0.1 nm. *ISEC*. home-assembled apparatus available at the Institute of Chemical Process Foundamentals, Czech Academy of Sciences (Prague-Suchdol). Basic operations and choice of steric probes are described in Ref. [8]. TG analyses were carried out with a Termogravimetric System Perkin-Elmer.

2.3. Samples preparation for TEM

Some samples were obtained by mechanical milling of the as-prepared solid sample and subsequent dispersing in ethanol with a ultrasonic bath for 0.5 h. One drop of the so obtained suspension was brought onto a carbon-coated copper grid, dried at room temperature and then put into the microscope.

2.4. Samples preparation for XRMA

As prepared materials are mixed with the resin precursor Araldite CY212 and subsequently spread on suitable glass supports to obtain a round-shaped "flat cake", ca. 1 cm in diameter and ca. 0.2 mm thick. After the solidification of the mixture, the sample was polished to such an extent to make observable a number of sections of catalyst particles.

2.5. Syntheses

The synthetic procedure to functional resins is described in various previous papers from these Laboratories. The reader is particularly referred to Ref. [4]. The only innovation that has been recently introduced is the washing procedure of the ground and sieved materials, i.e. a thorough treatment of the crude resin with a suitable solvent in a Soxhlet apparatus along 24 h, followed by conventional drying at 7.0×10^{-2} bar, 60 °C for 24 h. *Preparation of ADE*. A homogeneous mixture of ACN, 1.78 g, EDMA, 0.89 g and DMAA, 7.33 g produced a pale yellow transparent rod (9.62 g) and 380 mg of a liquid phase, with an estimated yield in solid material equal to 96%. *Irradiation conditions*. 15 cm from the ^{60}Co source at 15 °C for 24 h. Total dose is equal to 10 kGg. The rod is broken manually after 3 days of swelling in methanol. After drying at room temperature, the particles are finely ground with an IKA A10 impact grinder and subsequently washed with THF in a Soxhlet for 24 h. After drying at room temperature under vacuum, the resin mass is sieved to 180–400 μm. Anal. Calc. % (found): C, 61.90 (59.25); H, 5.34 (8.56); N, 15.07 (13.30). *Metallation of ADE* is carried out in water (ca. 20 ml) at room temperature for ca. 70 h upon letting suitable amounts of Na_2PdCl_4 to react with pre-swollen ADE (ca. 1 g) under moderate stirring, to reach –CN/Pd molar ratios equal to 40.1, 17.8 and 2.0, respectively. In all cases the weight percentages of Pd incorporation are remarkably almost identical, i.e. 1.64 (20.9:1.0), 1.72 (17.8:1.0) and 1.70 (2.0:1.0). The reduction of Pd^{II} to Pd^0 is carried out as follows: 10 ml water, ca. 200 mg of Pd^{II}/ADE, $NaBH_4$ (10:1 molar excess over Pd^{II}) under vigorous stirring at 0 °C or 50 °C, 30 min reaction time. After filtration, the black materials are dried at 60 °C, at 7.0×10^{-2} bar for 24 h and stored in the laboratory atmosphere.

2.6. Catalytic tests

Hydrogenation of cyclohexene. the tests were carried out in a glassy reactor fixed in a shaken stainless steel cylinder of the volume of 15 cm^3 able to operate under constant pressure conditions (6 bar in this case). The progress of the reaction was monitored upon direct measuring the consumed dihydrogen as far as 100% conversion into cyclohexane. Reagents concentrations data are reported in the captions of Fig. 7. Recycling tests were comfortably carried out upon withdrawing the reacted solution without removing the used catalytic material (this operation was particularly easy thanks to the higher specific weight of all employed catalyst). The test of the residual activity persisting in the liquid phase (after the first run) was carried out upon mixing 2 ml of the decanted final solution with 2 ml of a 1 M cyclohexene methanol solution and repetition of the standard procedure (see above).

2.7. Oxidation catalytic tests

Catalytic tests. *Oxidation of benzyl alcohol*: the tests were carried out in a classic 50 ml glass batch, stirred reactor. 103 mg of catalyst were suspended in 1.3 ml water containing 135 mg K_2CO_3 (0.75 M) [6] 100 μl benzyl alcohol and 100 μl *n*-dodecane as internal standard in a 50 ml glass balloon. Under a feeble oxygen stream (1 bar), the system was brought to 100 °C, under moderate stirring. After 90 min, the final mixture was treated with 3× 10 ml dichloromethane and the organic extract was analyzed with GC. *Oxidation of n-butanol*: 114 mg of catalyst were suspended in 5.0 ml water containing 138 mg K_2CO_3 (0.2 M) [6], 100 μl *n*-butanol and 100 μl *n*-dodecane as internal standard. The pure oxygen pressure was adjusted to 3 bar and the obtained suspension was kept under moderate stirring for 1.5 and 40 h. The course of the reaction was evaluated as described above.

3. Results and discussion

Resin ADE is obtained upon γ-rays-sustained co-polymerisation of a homogeneous mixture of *N*,*N*-dimethylacrylamide (DMAA) and acrylonitrile (AN) in the presence of ethylene-dimethacrylate (EDMA) as the cross-linker, 4 mol%, at room temperature (Table 1).

As expected from previous experience [7], polymerisation yield is near to 100%. The primary structure of ADE is sketched in Fig. 2.

The experimental elemental composition is acceptable for C and N (see Section 2). It is poor for H, but ADE is likely to be contaminated by absorbed solvents (see below TGA).

TGA profile (Fig. 3) reveals in fact some contamination by relatively low-boiling impurities and the expected thermal depolymerisation is seen to occur in the 350–450 °C temperature range.

The nanostructure of ADE-swollen alternatively in water and THF was investigated with inverse steric exclusion chromatography (ISEC) [8–10]. ISEC is the most powerful instrumental

Table 1
Molar percentages of DMAA, AN and EDMA in the synthesis of ADE

DMAA	ACN	EDMA
0.0654 mol	0.0270 mol	0.0040 mol
67.84 mol%	28.01 mol%	4.15 mol%

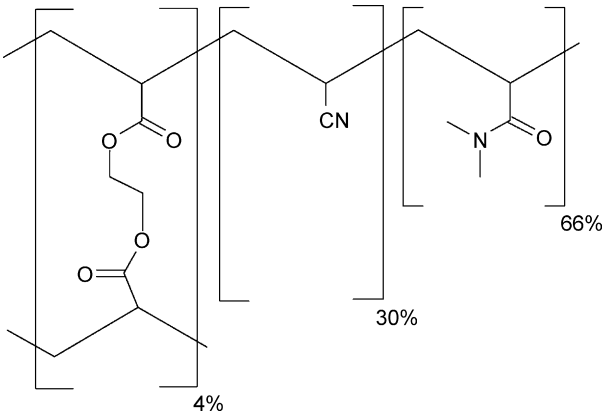

Fig. 2. Primary structure of resin ADE (3.39 mequiv./g of –CN).

analytical tool for depicting the morphology of swollen functional resins at the nanometer scale. This technique provides detailed information on the nanometer scale morphology of a given resin, after its swelling in a convenient liquid medium. It is based on measurements of elution behaviour of standard solutes with known effective molecular size on column filled with the investigated material at conditions when the elution is influenced exclusively by the (nano)morphology of the stationary phase. Similarly to in the case of the other porosimetric methods, mathematical treatment of the elution data allows one to obtain information on the morphology of the investigated material using a simple geometrical model. It is now established that for description of the morphology of swollen polymer gels the best suitable tool is the so-called Ogston's model [11] depicting pores as spaces between randomly oriented solid rods. This geometry, albeit a substantially simplified description of the morphology of swollen polymer networks, provides a fair description of both the intensive parameters (polymer chain densities) and extensive properties (specific volumes of variously dense polymer fractions). The density of the polymer fraction is expressed in units of length per unit of volume. In a real polymer framework we may detect fractions with the density from about 0.1 nm nm^{-3}, representing an extremely expanded cross-linked polymer to 1.5 nm nm^{-3} characterizing a denser polymer matrix

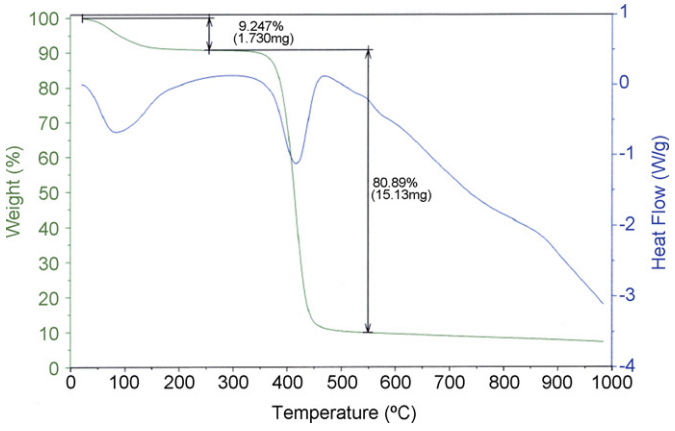

Fig. 3. TGA profile of resin ADE (heating rate is 10 °C min^{-1}). Courtesy Dr. G. Pace.

Table 2
ISEC determined morphology of ADE swollen in water and THF expressed in terms of the Ogston model

Fraction density (nm nm^{-3})	Fraction volume in the water-swollen state (cm^3/g)	Fraction volume in the THF-swollen state (cm^3/g)
0.1	0.02	0.00
0.2	0.10	0.00
0.4	0.00	0.00
0.8	0.20	0.00
1.5	1.45	0.85

into which even the smallest molecules penetrate with great difficulties. Results of this morphology characterization are shown in Table 2.

ISEC investigation alternatively in aqueous and organic environment succeeds in the separate characterization of hydrophilic and lipophilic domains in the same polymer [12]. Thus, in resin ADE the observed differences in the morphologies of the polymer swollen in water and THF are the likely consequences of the differences in the solvation of ACN-depleted domains, mainly composed of DMAA and EDMA and of ACN-rich domains that exhibit a relatively greater affinity for THF. ADE appears to be altogether mainly hydrophilic in nature as shown by its swollen added volume—SAV [13] that is in water about 1.51 ml g^{-1} versus only 0.62 ml g^{-1} at room temperature, in acetonitrile.

IR spectra (KBr disk) reveal a single ν_{CN} band at 2237 cm^{-1} due to free nitrile groups. SEM analysis reveals the expected glassy structure of dry gel-type resins [10] down to 10,000×.

Resin ADE, after swelling in water, is seen to behave as a reasonable macromolecular ligand towards aqueous Pd^{II} (Eq. (1)). This observation is not surprising in view of the well documented ability of the CN group of nitriles to act as good ligands towards Pd^{II} [14]. Evidently, the swelling makes the acrylic component accessible for metal co-ordination of ionic species. The simplest stoichiometry we can imagine is depicted below (Eq. (1)):

$$\text{Ⓟ-CN}_{(aq)} + PdCl_4^{2-}{}_{(aq)},\ 2Na^+_{(aq)} \rightarrow \text{Ⓟ-CN-PdCl}_3\urcorner^- Na^+ + Na^+_{(aq)} + Cl^-_{(aq)} \quad (1)$$

The metallation of ADE was carried out under various conditions differing in the value of the initial ratio between the moles of –CN ligating sites "offered" to the metal centre, and the moles of Pd^{II}. Remarkably, all three experiments carried out with ratios equal to 20.9, 17.8 and 2.0 lead to the same level of incorporation of Pd^{II} (ca. 1.7%, w/w)! Consequently, we admit that only a well defined relatively small molar fraction of –CN groups is actually capable of co-ordinating the Pd^{II} centers and we speculate that the macromolecular complex should be depicted according to the following notation (Scheme 2).

If this is the case, we conclude that *only* 0.16 mequiv./g of CN– groups are available for metal co-ordination (see later). In the macromolecular complex, the ν_{CN} band at 2237 cm^{-1} due to free nitrile groups is accompanied by a well defined, albeit weaker single band at 2295 cm^{-1} (Fig. 4) that can be safely attributed to the little fraction of nitrile groups that is involved in

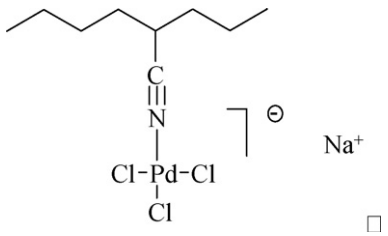

Scheme 2. Proposed structure for the molecular complex Ⓟ-CN-$PdCl_3^-Na^+$.

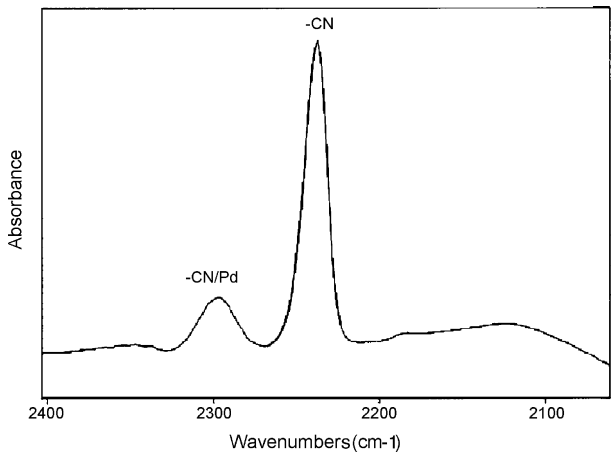

Fig. 4. IR spectrum of Pd0/ADE as KBr disk.

metal co-ordination. The involvement of more than one –CN ligating site in the co-ordination sphere of the metal centre appears to be very unlikely owing to the consequent proximity of two (or more) polymer chains in the same metal co-ordination sphere.

XRMA analysis (Fig. 5) reveals that the dispersion of palladium through the body of the resin particles turns out to be *macroscopically* homogeneous in nature.

When Ⓟ-CN-$PdCl_3^-Na^+$ is treated with $NaBH_4$ in water at 0 and 50 °C under vigorous stirring, the very rapid reduction of Pd^{II} takes place. The idea of employing two rather different temperatures stems from the circumstance that the difference in temperature might affect the size of Pd^0 nanoclusters [15]. The reaction is seen to occur in a few seconds at 50 °C and in ca. 1 min at 0 °C, with gas evolution and the production of black materials hereafter coded as Pd^0/ADE.

Both metal–polymer nanocomposites were examined with TEM as submicrometer-sized particles. The first observation is that reduction temperature does not seem to affect the TEM pattern. The second one is that Pd^0 nanoclusters do not appear as well isolated, size-controlled entities as it is usually observed with our Pd^0/resin and Au^0/resin nanocomposites, in which resin stands for the resins shortly depicted in the Introduction section. On the contrary, they appear as roughly spherical "clouds", featured by diameters ranging from 50 to 100 nm, built up with numerous 3–5 nm large nanoclusters (Fig. 6).

This unusual distribution of the metal nanoclusters is explicable on the basis of a two-phase morphology of ADE composed of compact poly-ACN nanospheres of which only the "surface" (*vide infra*) is available for Pd^{II} co-ordination. These nanospheroidal domains are therefore expected to be surrounded by the remaining DMAA–EDMA polymer gel. This inhomogeneous composition of the overall polymer framework could be produced by polymerisation-induced phase separation, promoted by the association of both ACN monomer molecules and the growing chains. The metallation experiments herein described, show that for interaction with Pd^{II} centers only 0.16 mequiv./g of the nitrile groups are available, which is about 5% of the acetonitrile units contained in ADE polymer. Upon considering the approximate density of poly-ACN as about 1 g/cm^3 we can estimate that one monomer unit of ACN occupies a cubic space with the edge length equal to 0.44 nm. By numerical simulation it can be shown that a sphere composed of units of this size and having 5% of these units in its surface layer would have the diameter of about 50 nm. This figure is in fact in reasonable agreement with the size-range of the spherical "clouds" of metal nanoparticles observed in TEM pictures (Fig. 6).

The metal nanoparticles at the surface (*vide infra*) of the poly-ACN microspheres are formed in fact within the swollen DMAA–EDMA gel domains and their size then should be related to the water-swollen gel morphology as characterized by ISEC. The morphology description using the Ogston model presented in Table 2 is for polymer materials the most suitable geometrical approximation but the polymer chain concentration parameter does not provide direct information about the effective size of the cavities in the polymer network. From the purely mathematical point of view, with essentially the same accuracy, it is possible to use also the conventional cylindrical pore model,

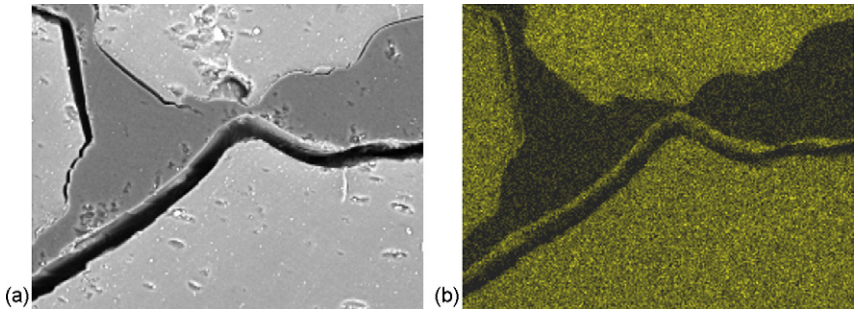

Fig. 5. (a) SEM pictures of the same sample: darker fields correspond to araldite (see Section 2) and to occasional empty elongated spaces formed during the drying of the sample. (b) XRMA of three sections of Ⓟ-CN-$PdCl_3^-Na^+$ Na^+: resolution power is ca. 0.5 μm. Courtesy of Dr. L. Tauro and of Dr. M. Favaro.

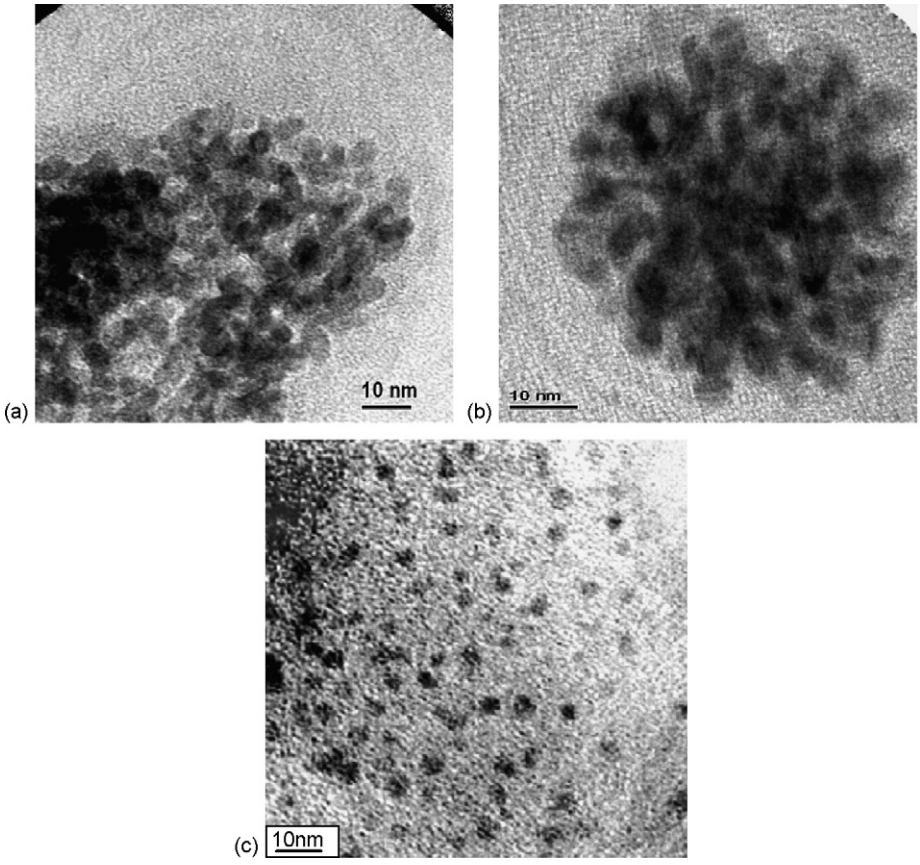

Fig. 6. (a) TEM micrographs of materials Pd^0/ADE-0 (obtained at 0 °C) and (b) Pd^0/ADE-50 (obtained at 50 °C); (c) TEM micrograph of a typical M^0/resin nanocomposite [16] prepared by us with our TCS strategy (see text).

commonly employed for the characterization of solid porous materials [8]. However, as this model relies on a geometry that is not directly related to the physical reality of the polymer framework, the cylindrical pore model gives good assessment of the effective pore sizes but its estimation of pore volume is incorrect. However, for investigating on the factors affecting the formation of metal nanoclusters inside of the swollen polymer matrix, the effective size of the "cavities" used in the templating molds is much more important than their specific volume (see Table 3).

In the water-swollen ADE resin, statistically prevail pores with a diameter equal to 0.5, 2.0 and 4.0 nm. According to our TCS model [1], we do expect that the generation of Pd^0 nanoclusters upon reduction of pre-co-ordinated Pd^{II} centers in water leads to Pd^0 nanoclusters featured by a ca. 4 nm diameter, again in agreement with the TEM observation (Fig. 6).

Table 3
ISEC determined morphology of ADE swollen in water expressed in terms of the cylindrical pore model

"Cylindrical pores" diameter (nm)	Pore volume in water-swollen polymer (cm^3/g)
12.0	0.02
8.0	0.00
4.0	0.16
2.0	0.83
1.0	0.00
0.5	2.44

3.1. Catalytic behaviour

3.1.1. Hydrogenation of cyclohexene

The activity of Pd^0/ADE is tested in a model reaction, in methanol under moderate P and T conditions. We considered useful comparing its behaviour with that of a classic Pd^0/Al_2O_3 catalyst prepared by the incipient-wetness impregnation of the support (gamma alumina, Aldrich, $s_{BET} = 164\ m^2/g$), calcined and reduced in hydrogen and of an innovative one manufactured by Reaxa Ltd. (Manchester) and commercialised by Aldrich, i.e. Pd^0/EnCat. In this last catalyst, the support is a functional gel-type resin somehow related to our ADE support [17].

The catalytic behaviours of Pd^0/ADE, Pd^0/EnCat and Pd^0/Al_2O_3 are illustrated in Fig. 7a–c (see captions for the conditions).

Fig. 7 illustrates an evaluation of the relative catalytic activity of Pd^0/ADE with respect to a classic catalyst such as Pd^0/Al_2O_3 and an innovative one such as Pd^0/EnCat (EnCat = commercially available gel-type polyurea) [17]. Moreover, Fig. 7d exhibits the relative resistance of the three catalysts towards "leaching" of active material into the surnatant.

The major conclusions stemming from the overall results are the followings:

(A) As prepared Pd^0/ADE does in fact contain some Pd^{II} that undergoes complete reduction after ca. 10 min.

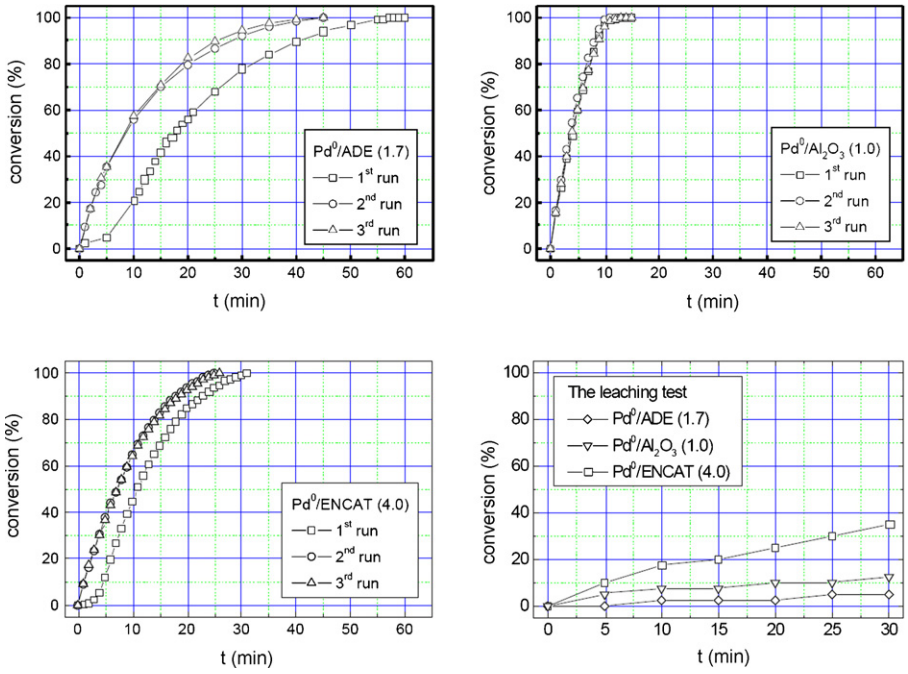

Fig. 7. Conversion curves from catalytic tests carried out with the as prepared (the first run) and recycled catalysts (second and third runs) and results from the leaching test. Numbers in brackets denote palladium percentage in a dry form of the catalyst. One molar solution of cyclohexene in methanol at the start, volume of the reaction mixture, 6 cm^3, analytical concentration of palladium 3.0×10^{-3} M, 0.6 MPa pressure in the system. In the leaching test 2 ml of the reaction mixture from the first run and 2 ml of 1 M cyclohexene in MeOH were mixed and used for catalytic tests.

(B) The activity profiles of Pd^0/ADE and of Pd^0/EnCat are fairly similar and suggest good accessibility of the catalytic centres.
(C) All the catalysts are nicely re-usable.
(D) Leaching of active material associated with catalyst use is very small for Pd^0/ADE and for Pd^0/Al_2O_3. Leaching is significant for Pd^0/EnCat.
(E) The very peculiar distribution of Pd^0 nanoclusters inside the polymer framework of ADE does not represent any drawback as far as the catalytic productivity of Pd^0/ADE is concerned.

3.1.2. *Oxidation of benzyl alcohol and of n-butanol*

The catalytic activity of Pd^0/ADE was tested in the oxidation of alcohols with molecular oxygen in water. The remarkable catalytic potency of Pd^0 in this important type of reaction has been recently illustrated by Uozumi and Nakao [18] upon employing Pd^0 dispersed on an amphiphilic resin and by Kaneda and co-workers [19] who utilized a Pd^0/hydroxyapatite catalyst. We also employed recently the chemoselective oxydation of *n*-butanol to *n*-butanal to test the catalytic activity of some Pd^0/hydrophilic resin catalysts [6].

In this investigation we choose benzyl alcohol and *n*-butanol as paradigms of aromatic and of aliphatic alcohols. The results are collected in Table 4. The conditions are close to those of Ref. [16].

It is seen that our catalyst is neither particularly active nor excitingly selective towards the formation of aldehyde. As expected from Refs. [15,16], the oxidation of benzyl alcohol to aldehyde is appreciably more selective than the oxidation of *n*-butanol to *n*-butanal. However, we wish to stress the circumstance that our new catalyst exhibits an interesting dual catalytic activity, i.e. in alkene hydrogenation and aerobic alcohol oxidation, i.e. a behaviour similar to that observed by Uozumi and co-workers [20a], upon employing an amphiphilic resin-supported nanostructured Pd^0/resin catalyst, and by Park

Table 4
Oxidation of benzyl alcohol and of *n*-butanol with Pd^0/ADE in water

Entry	Substrate	Reaction mixture (mol%)	Remarks
1[a]	Benzyl alcohol	Benzyl alcohol 92.2, benzaldehyde 7.8, benzoic acid 0.0	First run, after 1.5 h
2[a]	Benzyl alcohol	Benzyl alcohol 87.8, benzaldehyd 5.8, benzoic acid 6.4	Second run with recycled catalyst, after 6.5 h
3[a]	Benzyl alcohol	Benzyl alcohol 83.4, benzaldehyd 5.8, benzoic acid 10.8	Third run with recycled catalyst, after 6.5 h
4[b]	*n*-Butanol	*n*-Butanol 97.7, *n*-butanal 0.7, *n*-butanoic acid 1.6	Single run after 1.5 h
5[b]	*n*-Butanol	*n*-Butanol 84.0, *n*-butanal 1.3, *n*-butanoic acid 14.7	Single run after 40 h

[a] 103 mg of catalyst, 1.3 ml water containing 135 mg K_2CO_3 (0.75 M), 100 μl benzyl alcohol and 100 μl *n*-dodecane at reflux; 1 bar O_2; mol substrate/mol base = 1/1, mol substrate/mol Pd = 100/1.
[b] 14 mg of catalyst, 5.0 ml water containing 138 mg K_2CO_3 (0.2 M), 100 μl *n*-butanol and 100 μl *n*-dodecane; 3 bar of O_2, in a sealed reactor; mol substrate/mol base = 1/1, mol substrate/mol Pd = 100/1.

and co-workers in 2004 [20b], upon using a $Pd^0/Al(OH)_3$ catalyst.

4. Conclusions

Poly-acrylonitrile (30 mol%)–*N*,*N*-dimethylacrylamide (66 mol%)–ethylenedimethacrylate (4 mol%) turns out to be a somewhat peculiar resin in which the acrylonitrile component forms separate highly dispersed spherical nanodomains. In TEM pictures their existence is revealed by a "staining" effect caused by metal nanoclusters generated by reduction of Pd^{II} centers sorbed on the surface of the poly-acrylonitrile-rich domains. The Pd^0 nanoparticles decorate mainly spheroidal 50–100 nm domains dispersed in a swellable poly-acrylamide gel and exhibit an appreciable catalytic activity in the hydrogenation of cyclohexene. Pd^0/ADE reveals in fact an activity that is comparable with that of the commercially available catalysts Pd^0/alumina and of Pd^0/EnCat. Its resistance to "leaching" of active material (see above) is better than that of Pd^0/EnCat and comparable to that of Pd^0/Al_2O_3.

Acknowledgements

We thank Dr. L. Tauro and Dr. M. Favaro for XRMA measurements. Dr. G. Pace for the TGA measurements and Dr. S. Lora for assistance in the preparation of the functional resin. We are also grateful to CIGS, University of Modena, Italy, for the TEM analysis.

References

[1] B. Corain, K. Jerabek, P. Centomo, P. Canton, Angew. Chem. Int. Ed. 43 (2004) 959.
[2] A. Biffis, A.A. D'Archivio, K. Jeràbek, G. Schmid, B. Corain, Adv. Mater. 12 (2000) 1909.
[3] F. Artuso, A.A. D'Archivio, S. Lora, K. Jeràbek, M. Kralik, B. Corain, Chem. Eur. J. 9 (2003) 5292.
[4] M. Kralik, V. Kratky, M. De Rosso, M. Tonelli, S. Lora, B. Corain, Chem. Eur. J. 9 (2003) 209.
[5] B. Corain, C. Burato, P. Centomo, S. Lora, W. Meyer-Zaika, G. Schmid, J. Mol. Catal. A: Chem. 2245 (2004) 189.
[6] C. Burato, P. Centomo, G. Pace, M. Favaro, L. Prati, B. Corain, J. Mol. Catal. A: Chem. 238 (2005) 26.
[7] B. Corain, P. Centomo, S. Lora, M. Kralik, J. Mol. Catal. A: Chem. 204/205 (2003) 755.
[8] K. Jerabek, Cross evaluation of strategies in size-exclusion chromatography, in: M. Potschka, P.L. Dubin (Eds.), ACS Symposium Series 635, American Chemical Society, Washington, DC, USA, 1996, pp. 211–224.
[9] (a) K. Jerabek, Anal. Chem. 57 (1985) 1595;
(b) K. Jerábek, Anal. Chem. 57 (1985) 1598.
[10] B. Corain, M. Zecca, K. Jerabek, J. Mol. Catal. A: Chem. 177 (2001) 3.
[11] G. Ogston, Trans. Faraday Soc. 54 (1958) 1754.
[12] K. Jerabek, L. Hanková, A. Revillon, Ind. Eng. Chem. Res. 34 (1995) 2598.
[13] K.W. Pepper, D. Reichenberg, D.K. Hale, J. Chem. Soc. (1952) 3129.
[14] R. Michelin, M. Mozzon, R. Bertani, Coord. Chem. Rev. 147 (1996) 299.
[15] T. Teranishi, M. Miyake, Chem. Mater. 10 (1998) 594.
[16] B. Corain, P. Guerriero, G. Schiavon, M. Zapparoli, M. Kralik, J. Mol. Catal. A: Chem. 211 (2004) 237.
[17] (a) C.K.Y. Lee, A.B. Holmes, S.V. Ley, I.F. McConvey, B. Al-Duri, G.A. Leeke, R.C. Santos, J.P. Seville, Chem. Commun. (2005) 2175;
(b) S.V. Ley, C. Mitchell, D. Pears, C. Ramarao, J.Q. Yu, W. Zhou, Org. Lett. 5 (24) (2003) 4665;
(c) J.Q. Yu, H.C. Wu, C. Ramarao, J.B. Spencer, S.V. Ley, Chem. Commun. (2003) 678;
(d) S.V. Ley, C. Ramarao, A.L. Lee, N. Ostergaard, S.C. Smith, I.M. Shirley, Org. Lett. 5 (2) (2003) 185;
(e) S.V. Ley, C. Ramarao, R.S. Gordon, A.B. Holmes, A.J. Morrison, I.F. McConvey, I.M. Shirley, S.C. Smith, M.D. Smith, Chem. Commun. (2002) 1134;
(f) C. Ramarao, S.V. Ley, S.C. Smith, I.M. Shirley, N. DeAlmeida, Chem. Commun. (2002) 1132.
[18] Y. Uozumi, R. Nakao, Angew. Chem. Int. Ed. 42 (2003) 194.
[19] K. Mori, T. Hara, T. Mizugaki, K. Ebitani, K. Kaneda, J. Am. Chem. Soc. 126 (2004) 10657.
[20] (a) R. Nakao, H. Rhee, Y. Uozumi, Org. Lett. 7 (2005) 163;
(b) M.S. Kwon, N. Kim, C.M. Park, J.S. Lee, K.Y. Kang, J. Park, Org. Lett. 7 (2005) 1077.